Electrooculography Controlled Cursor (April 2021)

Samina Abdullah, Aidan Ahamparam, Elizabeth Dulzo, Samy Ismail
1. Department of Biomedical Engineering, University of Michigan,

***Abstract* - People with motor disabilities or those with amputated limbs may lack the capability to operate a computer using a standard mouse. In today's world, the use of a computer is necessary for everyday tasks and the inability to use a computer can be a huge burden. For such users, an alternate interface could be used to operate a mouse that does not require the dexterity of the average human but instead uses eye movement for cursor control. This report introduces the design of such an interface that uses Electrooculography (EOG) to control a computer cursor. Our system measures EOG signals from the right eye and were used to move a cursor to target points on the computer screen. Both vertical and horizontal movements were achieved and the cursor was able to be directed to both intermediate and extreme positions on the screen within an approximated 200 pixel region of error.**

Keywords - Electrooculography, LabVIEW, accessibility, accessible technology

I. Introduction

Electrooculography (EOG) is a technique for measuring the corneo-retinal standing potential that exists between the front and the back of the human eye. Four electrodes, one on each of the temples and one above the right eyebrow and one below the right eye, are used to acquire the EOG signal, and an additional electrode acts as the ground. Any kind of eye movement changes the orientation of the dipole which is recorded by the EOG. EOG is an extremely useful medical technique. It can be used to diagnose hereditary macular diseases, evaluating sleep/sleep stages, and for controlling mechanical devices. The goal of this lab is to build an EOG device that allows users to operate a computer via the movement of their right eye as opposed to hand motion. People with impaired motor function or dexterity are unable to control a computer's cursor through its intended interface, which restricts their ability to use computers. In this day and age, being able to use a computer is a necessary life skill. Therefore, this technology would be particularly useful for amputees, quadriplegics, and any individual unable to operate a typical mouse.

[1]

II. Experimental Setup

A. Electrode Placement

In order to acquire the EOG signals, electrodes were placed on 5 different locations on the face. Two electrodes were placed on sides of each eye to generate the horizontal lead, two were placed above and below the eye to generate the vertical lead, and lastly an electrode was placed on the center of the forehead to create a reference to ground.

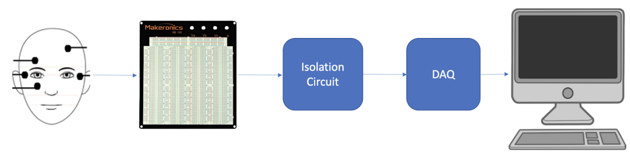

Figure 1. High Level Experimental Setup

B. Conditioning Circuit

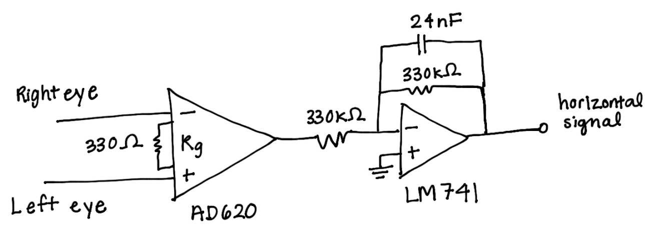

Figure 2. Horizontal Conditioning Circuit

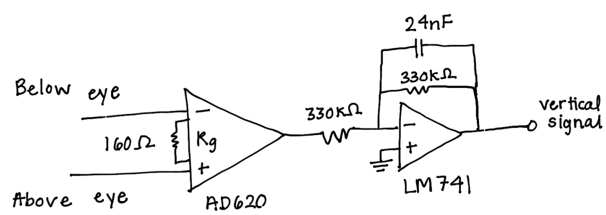

Figure 3. Vertical Conditioning Circuit

There were two signal conditioning circuits, one for the horizontal circuit and one for the vertical circuit. Figure 2 shows the schematic of the horizontal circuit, and Figure 3 shows a schematic of the vertical circuit. Both circuits consisted of an AD620 op amp used as a differential amplifier as well as a LM741 op amp used as a low pass filter. The gain on the op amp for the horizontal circuit was designed to be 150, and for the vertical circuit, 300. Both circuits were designed to have the same low pass corner frequency of 20 Hz. The following two tables show the ideal and actual measurements for the components in the circuit. Table I shows the measured values of the components in the circuit, and Table II shows the ideal values given the calculations shown below. R_G is the resistance across the AD620 for gain, R_1 is the resistance of the resistor that is not paired with a capacitor and is used to ensure unity gain across the filter. R_2 is the resistance of the resistor that is in parallel with the capacitor. C, is the capacitance of the capacitor in parallel with R_2 .

Table I. Measured Component Values

Measured Values of Components				
Device	AD620	LM741		
Component	R_G (Ω)	R_1 (kΩ)	R_2 (kΩ)	C (nF)
Horizontal	331	329.8	330.6	24.92
Vertical	159.84	329.96	329.88	23.55

Table II. Ideal Component Values

Ideal Values of Components				
Device	AD620	LM741		
Component	R_G (Ω)	R_1 (kΩ)	R_2 (kΩ)	C (nF)
Horizontal	331	330	330	24
Vertical	165	330	330	24

The ideal values of the components were calculated using two equations. For R_G, the resistor across the AD620, the value is calculated using the formula RG=49.4 kG-1. Where G for each circuit was defined above. To determine the capacitance to obtain a 20Hz low pass corner frequency, the equation C = 12Rfwas used where R was selected to be 330 kΩ, and f was 20Hz. The bode plots for the filters are shown below.

The error for the gain over the AD620 in the horizontal circuit was calculated to be 4.0% from the desired gain. We were not able to calculate the gain for the vertical circuit as we used a 5V power supply and the waveform generator could not produce a signal small enough where the output voltage from the AD620 would be below 5V.

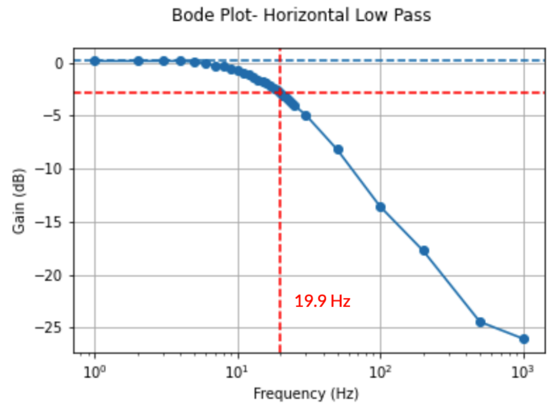

Figure 4. Horizontal LPF Bode Plot

Figure 4 contains the Bode Plot for the Horizontal circuit above shows a corner frequency of 19.9 Hz. Given the components, the expected corner frequency is 19.4 Hz. This yields an error of 2.6% from the expected corner and 0.5% from the desired corner.

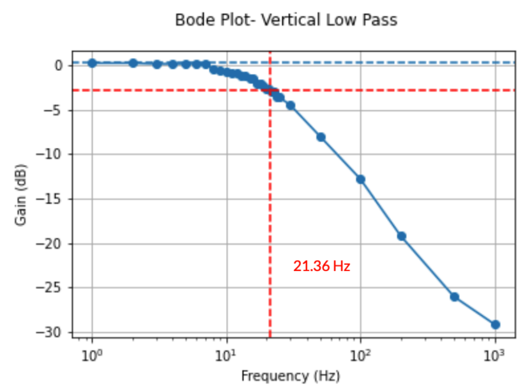

Figure 5. Vertical LPF Bode Plot

Figure 5 contains the Bode plot for the vertical circuit low pass filter. The corner frequency is 21.36 Hz and the expected corner given the components is 20.4 Hz. This yields an error of 4.7% from the expected cut off and 6.8% from the desired cutoff frequency

C. LabVIEW VI

The LabVIEW VI was designed to identify the incoming potentials from eye movement and convert them to horizontal and vertical cursor movements. A DAQ Assistant VI was used to split the incoming signal into two paths and then Select Signal VIs were used to identify the horizontal and vertical movement. Two Statistics VIs were used to identify the arithmetic mean for horizontal and vertical movement. These values were essentially the horizontal and vertical DC offsets so they were inputted manually into two Numeric Constants which were subtracted from the horizontal and vertical signals. These values were constantly fluctuating so they had to be updated at the beginning of each trial.

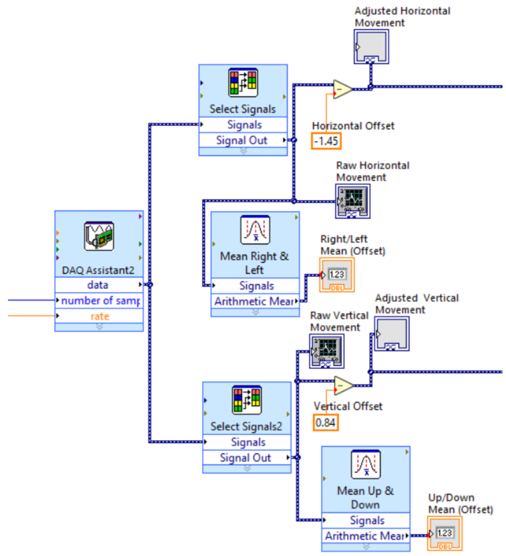

Figure 6.1. LabVIEW Block Diagram

Now that the DC offset was removed, Amplitude and Level Measurement VIs could be used to find the DC Means. The DC means were inputted into Formula VIs with the following equation: (Half Width/Height of Screen) + ((DC Mean) x (Scaling Value)). The width and height of the screen used for testing were 2550 and 1400 respectively. The scaling value was determined through calibration. The Formula VIs give the new horizontal and vertical cursor positions, which were inputted into a Windows Call Library Function VI that moves the cursor to these coordinates.

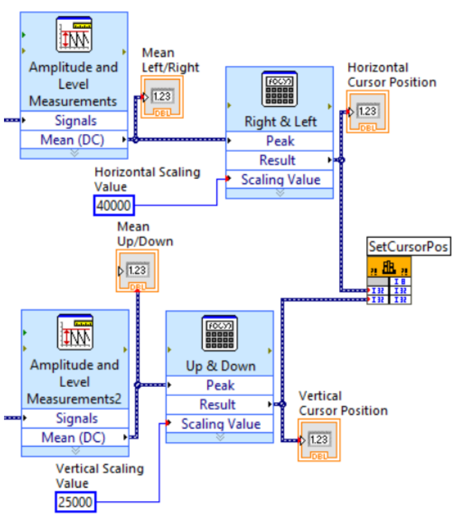

Figure 6.2. LabVIEW Block Diagram

D. Calibration

At the beginning of each trial, the participant was asked to look at the center of the screen so that the horizontal and vertical offsets could be recorded and the LabVIEW could be updated. The participant would then be asked to look to the four extreme locations (up, down, left, and right) so that the maximum DC Means could be determined. The following formula was used to determine the starting scaling values for each participant: (Half Width/Height of Screen) / |Maximum DC Mean|. These values were then adjusted via trial and error during testing such that the cursor could move the full height and width of the screen.

III. Results

First, the acquisition of our horizontal and vertical eye movement signals was validated. Figure 7 shows that our system is able to detect a change in voltage associated with left and right eye movement. For the first 4 units of time, the user looked straight. Then, the user was instructed to look right and left, corresponding with the decrease and increase in the amplitude relative to the straight baseline. Similarly, our system was able to detect up and down movement of the eye. However, we note that vertical movement produced a smaller change in amplitude, even with the conditioning circuit's higher gain.

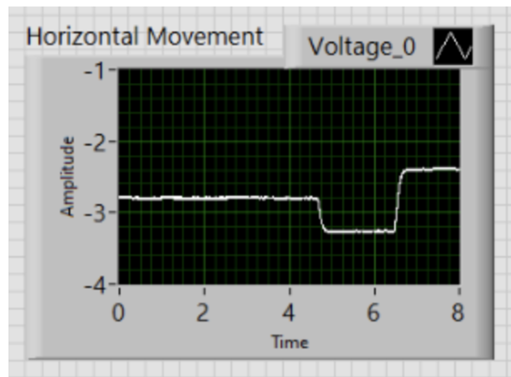

Figure 7. Horizontal Eye Movement Voltage Waveform Graph

Additionally, we note that the DC offset and eye movement voltage range was not constant throughout our experiments from user to user or over time. We tested our system for two different users. The first user's vertical offset was in the range of 0.4V to 1V with vertical extremes ranging from ±0.1V to ±0.15V. The second user's vertical offset was in the range of 0.5V to 0.8V with vertical extremes ranging from ±0.06V to ±0.2V. Both users had similar horizontal offsets ranging from approximately 1V to 2V. However, the first user had horizontal extremes ranging from ±0.7V to ±0.9V and the second user had horizontal extremes ranging from ±0.2V to ±0.4V.

Figure 8. Testing Eye Diagram

After validating the horizontal and vertical eye movement acquisition, the overall system was tested. First in our testing process, the system was calibrated to the user by measuring the voltage produced by straight eye position to determine the DC offset and the voltage produced by looking at the four edges of the screen to determine the Scaling Value. The eye diagram in Figure 8 was used to direct the user's eye movement in calibration and in testing our system's ability to move the cursor to different locations on the computer screen.

Our system successfully translated eye movement measured by an EOG signal to cursor movement. In experiments, users were able to move the cursor to extreme and intermediate horizontal values as well as to the four corners of the screen, within a region of error. We estimate this region of error to be a 200 pixel radius from the edge of targeted X.

IV. Discussion and Conclusions

In result, we successfully built an EOG-controlled cursor using hardware and software to identify vertical and horizontal potential differences and convert these values into a cursor location. However, the system had some accuracy error as the cursor would often go to the general desired location but not the precise location. This accuracy error is most likely due to the fluctuating offsets that had to be updated frequently. Having to make the time-varying adjustments was one of the most complicated aspects of the project. Some other challenges that were faced during this project include tuning the conditioning circuit's gain to the appropriate sensitivity, balancing complexity and accuracy in the hardware design, and acquiring a strong vertical signal. Acquiring the vertical signal changes was more difficult than acquiring the horizontal signal changes due to the smaller "range of motion" that the human eye is capable of reaching in the vertical direction which produces a smaller change in voltage potential. Another experimental challenge was handling and preventing user fatigue.

V. Future Directions

There are a variety of future directions we could take to further develop and improve our EOG-controlled cursor device. The calibration process needs to be streamlined to be more robust so that it would need to be repeated less frequently. Because this device is intended for people who have difficulty using their hands, the calibration process would need to be performed via vocal commands, similar to how Apple's Siri or Amazon's Alexa function. A way to turn off and run the system using vocal commands is an additional future work. The current software design is specific to one screen size. Therefore, the system needs to be further developed and tested to be adaptable to different screen sizes. Additional experimentation is required to determine how the systems accuracy and usability is affected by different screen sizes. Finally, to accomplish complete cursor functionality, a way to click the mouse, possibly by blinking, should be integrated into our system.

Acknowledgment

The authors would like to thank the University of Michigan Department of Biomedical Engineering for funding this project and the BME 458 staff for assisting with the project.

References

[1] Abbas S.N., Abo-Zahhad M. (2017) Eye Blinking EOG Signals as Biometrics. In: Jiang R., Al-maadeed S., Bouridane A., Crookes P., Beghdadi A. (eds) Biometric Security and Privacy. Signal Processing for Security Technologies. Springer, Cham. https://doi.org/10.1007/978-3-319-47301-7_5

[2] Banerjee, Anwesha, et al. "Classifying Electrooculogram to Detect Directional Eye Movements." *Procedia Technology*, vol. 10, 2013, pp. 67–75, www.sciencedirect.com/science/article/pii/S2212017313004921, 10.1016/j.protcy.2013.12.338. Accessed 16 Oct. 2019.

[3] Creel, Donnell J. "The Electrooculogram." *Handbook of Clinical Neurology*, vol. 160, 2019, pp. 495–499, pubmed.ncbi.nlm.nih.gov/31277871/, 10.1016/B978-0-444-64032-1.00033-3. Accessed 30 Mar. 2021.

[4] "Electrooculogram." EyeWiki, 23 June 2019, eyewiki.aao.org/Electrooculogram.

[5] "Electrooculography - an Overview | ScienceDirect Topics." *Www.sciencedirect.com*, www.sciencedirect.com/topics/neuroscience/electrooculography.

[6] Huang, Eric Cole, Evan Mok and Alex, and Eric Cole Huang Evan Mok and Alex. EOG-Controlled Video Game. circuitcellar.com/research-design-hub/eog-controlled-video-game/. Accessed 23 Apr. 2021.

[7] Z. Hossain, M. M. H. Shuvo and P. Sarker, "Hardware and software implementation of real time electrooculogram (EOG) acquisition system to control computer cursor with eyeball movement," 2017 4th International Conference on Advances in Electrical Engineering (ICAEE), 2017, pp. 132-137, doi: 10.1109/ICAEE.2017.8255341.

[8] Ramkumar, S., Kumar, K. S., Rajkumar, T. D., Ilayaraja, M., & Shankar, K. (2018). A review-classification of electrooculogram based human computer interfaces.